Glass Transition Phenomena in Melt-Processed Polystyrene/Polypropylene Blends

Vivek Thirtha, Richard Lehman, Thomas Nosker
AMIPP Advanced Polymer Center, School of Engineering, 607 Taylor Road, Rutgers University, Piscataway, New Jersey 08854-8065

Blends of an amorphous and a semi-crystalline polymer—polystyrene and polypropylene, respectively—were prepared by melt processing in an extruder at 220°C. These polymers are known to be immiscible and the composite morphologies were characterized by electron microscopy and thermal analysis. Fine micron-scale morphologies, ranging from 0.5 to 20 microns were observed. Thermal analysis and dynamic mechanical analysis showed changes in both the polystyrene and polypropylene glass transition temperatures (T_g) over the composition range. The major effect was a sharp increase in polystyrene T_g with increasing polypropylene content in the blend. A T_g elevation of 5.5°C was observed at 85% polypropylene. The polypropylene T_g also increases with increasing polypropylene content, starting at a depressed value in discrete polypropylene domain environments and approaching the bulk polypropylene value after the phase inversion is crossed. Qualitative structural models are proposed based on spatial and mechanical interactions between the components. POLYM. ENG. SCI., 45:1187–1193, 2005. © 2005 Society of Plastics Engineers

INTRODUCTION

Immiscible polymer blends have been of considerable interest because of their inherent capability to combine complementary functionalities of the component systems [1]. Low cost, high value materials can be easily and inexpensively prepared from immiscible polymers if blends follow the rule of mixtures without compatibilizers.

The morphology of the blends and the subsequent interaction between the component phases is a critical feature of immiscible blends that has the ability to transform properties such as the melting temperature (T_m), glass transition temperature (T_g), and the degree of crystallization [2]. Linear glass transition variations have been observed in thin films of polystyrene by various researchers [3, 4]. The T_g of certain polymers in the physical form of thin films or nanoparticulates has been shown to decrease as a function of the film or particle dimension [5]. The authors attributed this to surface area/volume effects, although the small dimensions present in the nanoparticulates would certainly constrain the size of any polymeric entity, thus altering its structural behavior. Other studies reported a change in T_g of polyethylene terephthalate (PET) in a blend with polycarbonate. The T_g of PET in the blend was higher than that of the pure polymer. The presence of a rigid polycarbonate matrix as PET cools through its glass transition gives rise to a "wall" effect, causing the T_g of PET to increase [6]. The T_g of polybutadiene in polycarbonate/ABS blends was shown to decrease with decreasing ABS content. This was attributed to different thermal expansion coefficients of the polybutadiene particles and the surrounding matrix [7, 8].

Polystyrene/polypropylene (PS/PP) blends are attractive for their potential use as packaging materials due to their water vapor resistance [9], although there have been few papers dealing with such blends and their properties in the uncompatibilized form [2, 10, 11]. The T_g of polypropylene in a PS/PP blend has been shown to decrease with decreasing polypropylene composition, apparently due to the thermal expansion coefficient mismatch, while the T_g of polystyrene did not change [12]. Mucha [13] concurred that there are physical interactions between phases that cause the T_g of *a*PS and *i*PP to change in an *a*PS/*i*PP blend. Greco et al. [14] did not see a linear variation in the T_g with composition in PS/PP systems, but saw the T_g increase to a single higher value from the homopolymer value at a certain composition. They attributed this to the migration of low molecular weight species into the polypropylene phase.

Our laboratory has focused on combining immiscible polymers by melt processing. The blending of a glassy polymer with a semi-crystalline polymer, e.g., polystyrene/HD polyethylene, has produced materials that generally show rule of mixtures behavior but that also demonstrate an important synergy of blend properties at certain compositions [15]. This behavior has been attributed to the unique morphology at the phase inversion composition of the components. An enhanced mechanical interaction at the

Correspondence to: R. Lehman; e-mail: rllehman@rutgers.edu
Contract grant sponsor: New Jersey Commission for Science and Technology.
DOI 10.1002/pen.20387
Published online in Wiley InterScience (www.interscience.wiley.com).

interface is obtained due to the differential shrinkage of the constituent phases as they cool through crystallization and glass transition temperatures. Whereas much of the prior work deals with the morphology, mechanical properties, co-continuous behavior, and the crystallinity of the blends and the components, this study has focused specifically on the effect of the blend morphology and phase interactions on the T_g of the glassy phases present in the blends. The current work has examined blends of polystyrene and polypropylene with regard to morphology of the blends after extrusion, and the effect of composition on the T_g of the polystyrene and polypropylene.

EXPERIMENTAL

Materials and Processing

Commercially available polymers were used for this study. Polypropylene (isotactic) with a melt flow index of 0.7 g/10 min (2.16 kg at 230°C) was obtained from Chevron Phillips Chemicals (The Woodlands, TX), and GPPS7 polystyrene with a melt flow of 7.0 g/10 min (5 kg at 200°C) was obtained from GE Polymerland.

A full range of blends from 15 to 95% polystyrene by weight were prepared via melt processing in a 19 mm single screw extruder (CW Brabender Intellitorque Plasti-corder) with a 25:1 mixing screw at 220°C and 100 rpm. The temperatures in the three zones of the extruder were maintained at 220°C. For the dynamic mechanical analysis (DMA), rectangular specimens with compositions ranging from 10 to 90% polystyrene were injection molded with a Negri-Bossi v55-200, 55-ton injection molder.

Imaging

Specimens of extruded samples were cryo-fractured in liquid nitrogen to produce a virgin surface characteristic of the bulk morphology. Specimens with 50% polystyrene and less were etched with toluene to provide greater relief for the imaging process. The remaining compositions were not etched for fear of compromising the morphological integrity. All specimens were sputter coated with gold-palladium for 2 min to produce a conductive coating and imaged with a Leo-Zeiss Gemini 982 field-emission scanning electron microscope (FESEM).

Differential Scanning Calorimetry (DSC)

The glass transition of the blend components was studied using a Q1000 Differential Scanning Calorimeter (TA Instruments, New Castle, DE) operated in modulated DSC mode (MDSC). The MDSC technique increases the limit of detection of glass transition and also improves the statistical significance of the data. Furthermore, by separating the reversing and non-reversing heat flows, the method easily detects thermal events that are difficult to detect with conventional heat-flux DSC [16]. All DSC runs were conducted over the temperature range of −30°C to 230°C with a three part sequence that included modulated heat, modulated cool, and modulated reheat. The underlying heating rate and cooling rate was 3°C/min, and the modulation amplitude was ± 1.3°C, with a period of 40 sec. The reversing heat curve obtained by modulating the heating rate in the DSC was used for the T_g observation. Precise T_g values were obtained by measuring peaks on the derivative graph of the enthalpy vs. temperature curve. This method reduces error associated with T_g measurements using the onset-end intercept method.

DMA

DMA was performed in an AR-2000 rheometer (TA Instruments, New Castle, DE) operated in the rectangular solid torsion mode inside an environmental test chamber (ETC). The test samples were 48.0 × 12.7 × 3.4 mm and were tested over a temperature range of –50°C to 180°C at a rate of 2°C/min and a frequency of 1 Hz. Liquid nitrogen was used to generate low temperatures, as required, and was also used to precisely control temperatures during heating. The strains at the linear viscoelastic region (LVR) of each sample were determined before the temperature ramp tests, and were found to be between 0.01% and 0.03%. The maxima of the G″ curves were used as the measure of T_g.

RESULTS AND DISCUSSION

Co-continuity

The relationship between the phases in an immiscible polymer blend depends substantially on the volume fraction and viscosity of each phase. Clearly, when one phase is present in only small quantities, e.g., 5–10%, that phase will likely be a discontinuous phase in a matrix of the major phase. However, this relationship can be affected by the shear conditions of the forming process and the relative melt viscosities of the phases. Extrusion typically forms highly oriented structures where thin strands of even a minor phase can be continuous in the longitudinal direction, i.e., along the extrusion axis. Furthermore, co-continuity of phases depends on the relative viscosity of the two phases in addition to the volume fraction. A quantitative, empirical description of this relationship has been given by *Eq. 1* [17]:

$$\frac{\eta_A}{\eta_B} \cong \frac{\Phi_A}{\Phi_B} \tag{1}$$

where in a blend of A/B, η_A = viscosity of polymer A, η_B = viscosity of polymer B, Φ_A = volume fraction of polymer A, and Φ_B = volume fraction of polymer B.

Co-continuity is expected at a composition of approximately 40% PS-60% PP as evidenced by the melt flow

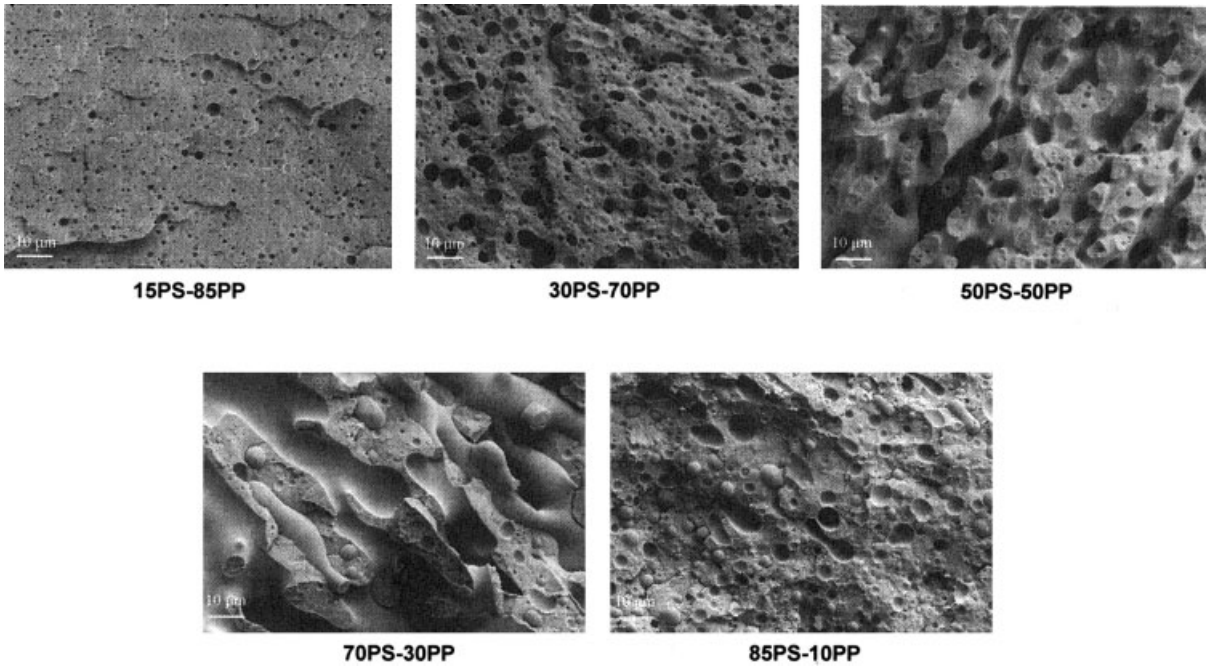

FIG. 1. Electron micrographs of polystyrene-polypropylene blends with 15, 30, 50, 70, and 85% polystyrene in polypropylene.

values and viscosity data, adjusting for shear rate and MFI force and temperature.

Morphology

The electron micrograph images of the extruded polystyrene-polypropylene blends with compositions 15% PS-85% PP, 30% PS-70% PP, 50% PS-50% PP, 70% PS-30% PP, and 85% PS-15% PP are shown in Fig. 1.

The 15%, 30%, and 50% PS specimens are etched, whereas the 70% and 85% specimens are not. The structure of blends over this composition range vary from small discrete regions of polystyrene, to co-continuous blends near the 50% composition, to phase inverted structures at higher polystyrene levels where the polypropylene is the minor phase. More specifically, in the 15% PS micrograph, the polystyrene can be seen as evenly distributed small inclusions that were removed by etching. A higher percentage of the etched phase is seen in the 30% PS micrograph, where the higher polystyrene percentage has caused coalescence of the melt droplets into bigger sizes, thus increasing its domain size. The 50% PS composition shows both phases to be mostly continuous, indicating proximity to phase inversion [18]. The 70% and 85% PS blends show a steady increase in the polystyrene and a decrease in the polypropylene phase, which appears in mostly dispersed form at 85%.

Glass Transition and Crystallization Effects

The values of the polystyrene glass transition for various blend compositions, as determined by the derivative peak method from the DSC reversing heat flow curves, are shown in Fig. 2. The T_g of polystyrene measured by DMA are shown in Fig. 3. The plot shows the loss modulus (G″) of the blends for polystyrene compositions ranging from 10% to 100%. The T_g is determined by the peak of the G″ curve. The T_g values from both thermal analysis (DSC) and mechanical analysis (DMA) are observed to shift from a value of ~100°C for 100%PS, to higher temperatures as the polystyrene concentrations decrease. Figure 4 is a composite graph that shows the change in polystyrene T_g in PS/PP blends over the composition range as determined by three methods, first DSC heat, second DSC heat, and by DMA. In this figure the T_g of polystyrene increases sharply with small

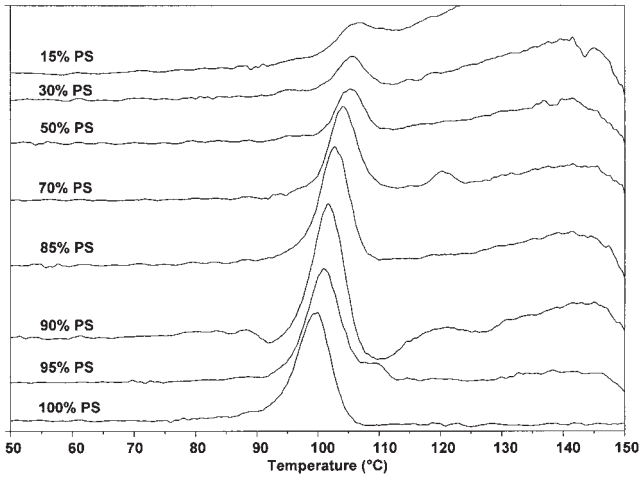

FIG. 2. Derivative of the reversible DSC heat curves for PS/PP blends near polystyrene T_g.

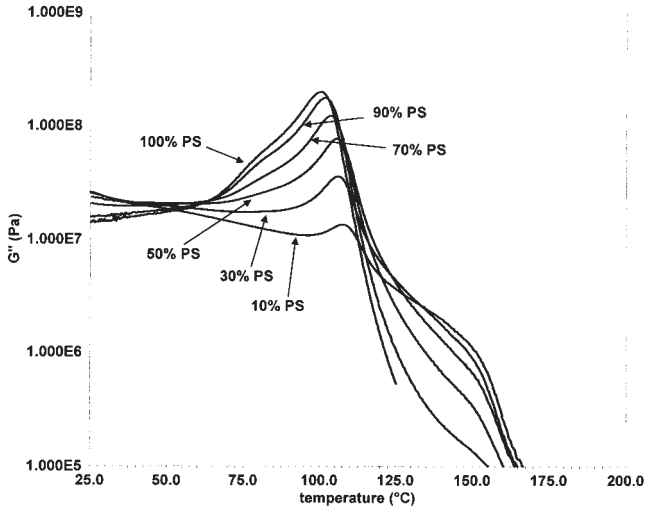

FIG. 3. DMA curves for PS/PP blends near polystyrene T_g.

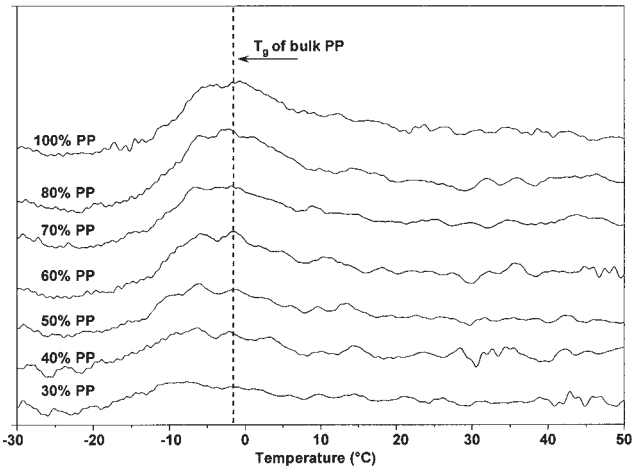

FIG. 5. Derivative of the reversible DSC heat curves for PS/PP blends near T_g of polypropylene.

additions of polypropylene with the greatest slope of the curve corresponding to the smallest amounts of polypropylene. As greater amounts of polypropylene occur in the blend, the slope of the curve diminishes. For blends with more than approximately 50% polypropylene there are only small changes in T_g of the polystyrene, and the T_g remains at the elevated level of ~106°C. The overall magnitude of the T_g shift is significant, about 6°C, as measured by both DSC and DMA. The second DSC heating cycle yielded data that are slightly greater than the first heating cycle, although the differences are small and insignificant. The T_g values measured by the three methods agree well and show similar trends.

In partially miscible polymer blends, the T_g of each component moves towards the T_g of the other component and a single intermediate T_g will form in a completely miscible blend. Since polystyrene and polypropylene are known to be immiscible, this effect should not be observed. Furthermore, it is interesting to note that the T_g of the polystyrene is *increasing* as polypropylene is added to the composition, opposite to the direction that would be expected if partial miscibility were occurring between the glassy polystyrene and the glassy portion of polypropylene. The curves in Fig. 2 also show that the onset points of all the T_g values are shifting and no broadening in the peaks occurs.

The T_g of the amorphous phase of the polypropylene also varied with blend composition, increasing with increasing polypropylene concentration. The effect is shown in DSC curves (Fig. 5), DMA graphs (Fig. 6), and a summary plot of all data (Fig. 7). The polypropylene DSC data show more scatter than the polystyrene data since the amorphous phase is only a fraction of the total polymer and because of the nature of this glass transition. The broad polypropylene derivative T_g curve (Fig. 5) makes identification of a single value of the transition more of a challenge. Nonetheless, the clear trend of DSC T_g data with composition and the good agreement with DMA T_g data are compelling evidence of

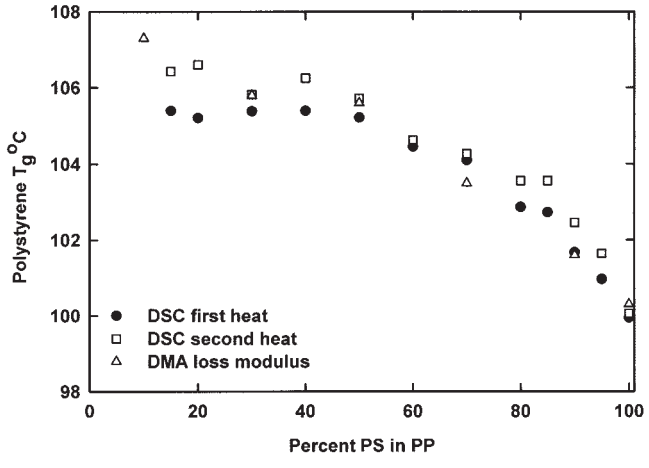

FIG. 4. Polystyrene T_g as a function of composition in PS/PP blends.

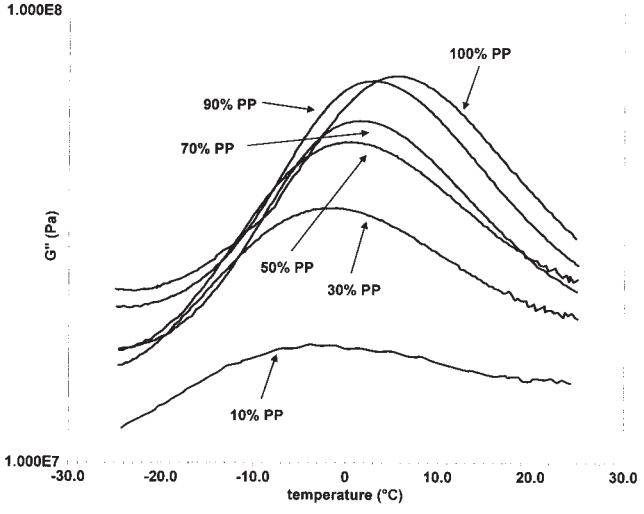

FIG. 6. DMA curves for PS/PP blends near polypropylene T_g.

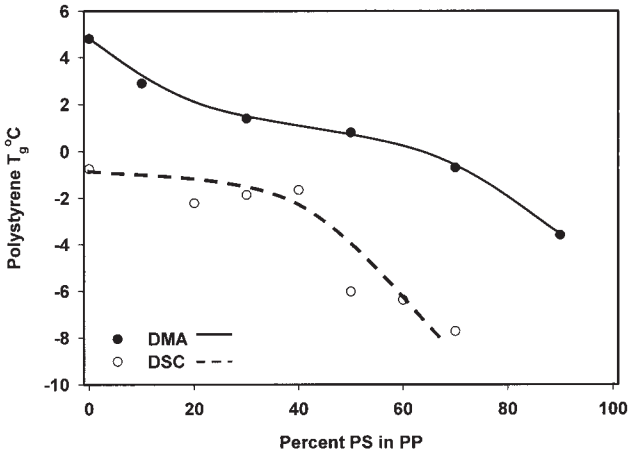

FIG. 7. Polypropylene T_g as a function of composition in PS/PP blends.

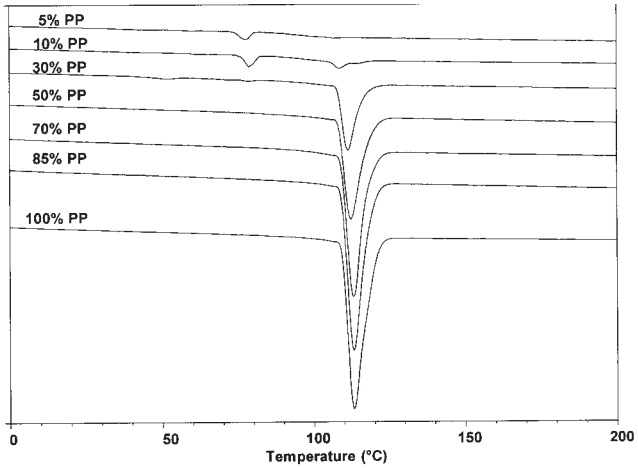

FIG. 9. Cooling curves for PS/PP blends.

the composition dependence of this transition. The T_g of polypropylene is clearly depressed on the high polystyrene side of the composition axis where polypropylene is present in discrete domains. When polypropylene is the continuous phase at low polystyrene concentrations, the T_g is essentially constant with composition, increasing only slightly as pure polypropylene is approached.

The melting behavior of the crystalline component of the polypropylene is shown in Fig. 8 as represented by the total heat flow curves of the blends. A subtle but statistically significant trend appears as the polypropylene melting point decreases with decreasing fraction of polypropylene in the blend below 50%. This effect, highlighted by a vertical reference line on the graph that helps illustrate the slight reduction in T_m of polypropylene compared to the neat polypropylene T_m (162.4°C), is greatest at the lowest polypropylene concentrations where polypropylene is present as small discrete domains surrounded by polystyrene. Figure 9 shows the total crystallization exotherms during the cooling scan of the blend samples. The crystallization temperatures (T_c) of the 30% PP to 100% PP samples are approximately 110°C. The 10% and 5% polypropylene samples show crystallization at lower temperatures, ~80°C. This behavior has been observed previously and is attributed to a change in the principal nucleation mechanism of polypropylene from heterogeneous to homogeneous, when the size of the dispersed polypropylene is below a critical dimension [19, 20].

The melting point reduction may result from an interaction between the glassy phase and the crystalline phase of the semicrystalline polymer [13]. However, this possibility is considered unlikely since the shift occurs not only as supercooling (Fig. 9), but also as a slightly depressed melting point (Fig. 8) that apparently results from the exceptionally fine crystallite distribution produced by homogeneous nucleation in small, isolated discrete polypropylene domains.

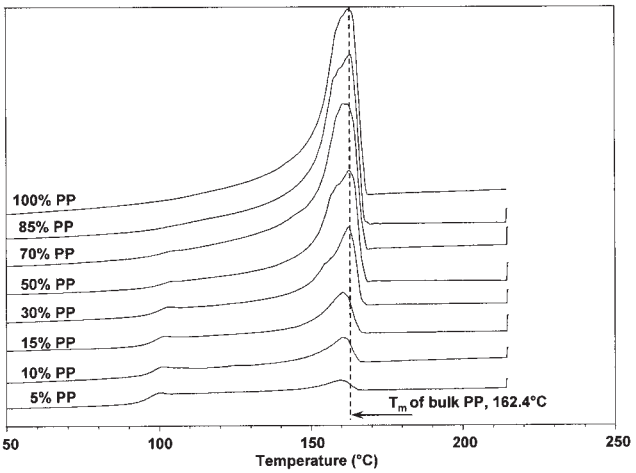

FIG. 8. Total heat flow DSC heat curves for PS/PP blends.

Mechanisms

Some aspects of the polystyrene T_g elevation are readily explained, whereas other aspects are more puzzling. At low concentrations of PS in a PP matrix the polypropylene will completely surround the dispersed polystyrene. If T_c is greater than T_g of the amorphous polymer, then the semicrystalline polymer will attempt to crystallize at T_c, with associated volume reduction, while the amorphous polymer is still in the liquid state. The liquid polymer will resist the volume contraction and will be under compressive stress with a resultant elevated T_g due to the well known pressure dependence of T_g [21]. This mechanism explains the T_g elevation in the polystyrene-dispersed region of the blend. The blends with 40–60% PP are approximately co-continuous and the morphologies are more complicated. In this region, which is characterized by frequent changes in the sign of curvature of the interfacial phase boundary, some of the polystyrene is surrounded by polypropylene and subject to the compressive stress T_g-raising mechanism noted above, but some is not. Such a transitional region is expected to show a reduction in the T_g elevation due to the

reduced amount of polystyrene phase subject to polypropylene compression, as shown in Fig. 4. At blend compositions higher than 60% PS the blend consists of dispersed PP in a PS matrix. Clearly, there is no stress imparted by the PP on the PS matrix in this composition region since polypropylene has higher thermal expansion than polystyrene and the dispersed domains will pull away from the surrounding polystyrene matrix upon cooling. Interestingly, a significant T_g elevation exists in this region. In fact, the slope of the curve ($\Delta T_g/\Delta$PP conc) is greatest here.

We believe the change of PS T_g with composition at high polystyrene concentrations, i.e., above the phase inversion, is due to physical constraints in the blend system. The presence of small dispersed points of polypropylene in a 95/5 PS/PP blend disrupts the molecular relaxation and cooperative mobility between structural units that is required during the glass transition process [22], thus resulting in a slightly higher T_g. At high temperature ($T >> T_g$) the rotation and vibration of the molecular units is highly energetic and generates substantial free volume and little cooperative motion between conformers is required, i.e., each unit can relax independent of its neighbors. However, as the temperature is reduced closer to T_g, the level of cooperative motion between conformers required to achieve the new lower temperature relaxed structure increases. Such cooperative motion requires some transient dilation of the structure to achieve this configuration. If such conformers are cooled in a constrained domain in the transformation range of the polymer, the restricted motion of the conformers will prevent them from relaxing to the volume and state corresponding to the T_g of the bulk polymer. Thus, the structure is set, i.e., T_g is established, at a higher temperature than would occur in unconstrained space. This theory is similar to that noted by Reinsch and Rebenfeld [6] in their work with PET/PC blends. A similar effect has been observed when polymers such as polystyrene, PMMA, polypropylene, and nylon-6 are blended with glass beads [23–25] in which the presence of highly dispersed glass beads increases the T_g of the matrix polymer. Apparently the inert glass particles are either pinning the polymer structure or otherwise generating immobilization zones that inhibit the relaxation processes necessary for the liquid to glass transition [26]. The polypropylene in the present blends can be likened to the solid glass beads in that they constrain the structure and alter T_g. Although the scale of the composite domains found in the studied blends is large ($\sim 3\ \mu$m) compared to the polystyrene molecule, the cooperative motion of conformer units near the glass transition can be affected by constraint volumes several orders of magnitude larger than the molecular size. As the polypropylene concentration increases, the disruption of the polystyrene matrix increases, thus generating a greater T_g elevating effect—precisely the behavior observed. This phenomenon extends, with increasing polypropylene concentration, into the co-continuous region and explains why two T_g are not observed for polystyrene in this region as would be expected by exclusive application of the compressive stress model. Effort continues in our laboratory on this topic and a more detailed experimental investigation is underway on a broader range of polymer pair compositions that is expected to reveal greater understanding of this phenomenon.

Although the above models appear to explain the observed behavior of the blends, we were interested in considering other possibilities. One such possibility that arose is the migration of additives from the commercial grade PS into the PP phase. The polystyrene selected for this study is so-called "crystal polystyrene," which traditionally has very few additives [27, J.D. Idol, personal communication]. Significant amounts of lubricants and other additives are unacceptable since they would reduce the clarity of molded specimens. Crystal polystyrene may contain low levels ($\sim$100 ppm) of certain antioxidants to prevent chain scission and molecular weight reduction. These antioxidants are hindered phenols, e.g., 2,6(di-tert-butyl)phenol and sometimes analogous hindered amines, both of which are anti oxidants but not plasticizers. Thus, strictly from a polystyrene composition perspective, the additive migration argument is considered unlikely. Further, such additive migration would quickly reach saturation and be limited by transport barriers at low polypropylene concentrations, e.g., 5%, precisely the region where the T_g curve has its greatest rate of change. Also significant is the trend of the polypropylene T_g data as measured by DSC and DMA (Figs. 5–7), which is quite similar to that of polystyrene, i.e., increasing with increasing polypropylene concentration. From a composition point at low polypropylene concentration, say 5%, an incremental increase in polypropylene will result in an increase in the T_g of both PS and PP. If additive migration were causing the PS T_g increase, then the increasing level of plasticizing additive that migrated into the polypropylene would result in a reduction, not an increase, in polypropylene T_g. Another issue that was explored was the possibility that the small amounts of atactic (amorphous) polypropylene (*a*PP) present in the polypropylene were becoming miscible with polystyrene and alloying with the major phase. This explanation was dropped since only minute amounts of impurity *a*PP are available at low polypropylene concentrations, and any alloy of the low T_g *a*PP ($T_g < 0$°C) and polystyrene would result in a lower alloy T_g, not a higher one.

SUMMARY AND CONCLUSIONS

Blends of the selected polystyrene and polypropylene polymers are immiscible over the entire compositional range and form dispersed blends near the neat component endpoints, co-continuous blends in the 40–60% region, and transition morphologies in between. The T_g of polystyrene shows elevated values compared to bulk T_g at all blend compositions, with the greatest effect at low polystyrene concentrations where polystyrene is the dispersed phase in a polypropylene matrix. Dispersed polypropylene phase pinning of the polystyrene matrix appears to be the responsible

mechanism for T_g elevation at high concentrations of polystyrene and may be an important contributing mechanism in the co-continuous region as well. At low polystyrene concentrations, compressive stress generated by the contracting polypropylene matrix appears to be the dominant mechanism in raising polystyrene T_g. The T_g of polypropylene follows a similar trend in these blends, increasing with increasing polypropylene content. The isolation of small polypropylene domains in polystyrene at low polypropylene concentrations results in a transition to homogeneous nucleation with a concomitant decrease in crystallization temperatures and a slight decrease in melting point.

ACKNOWLEDGMENTS

The authors wish to thank Professor James D. Idol for his excellent contributions to the research and to the manuscript, and TA Instruments for contributing equipment, support, and expertise to this effort.

REFERENCES

1. L.A. Utracki, *Polymer Alloys and Blends: Thermodynamics and Rheology*, Hanser, Munich (1989).
2. W. Wenig, H.W. Fiedel, and A. Scholl, *Colloid Polym. Sci.*, **168**, 528 (1990).
3. Q. Jiang, H.X. Shi, and J.C. Li, *Thin Solid Films*, **354**, 283 (1999).
4. J.A. Forrest, K. Dalnoki-Veress, J.R. Stevens, and J.R. Dutcher, *Phys. Rev. Lett.*, **77**, 2002 (1996).
5. Z. Zhang, M. Zhao, and Q. Jiang, *Physica B*, **293**, 232 (2001).
6. V.E. Reinsch and L. Rebenfeld, *J. Appl. Polym. Sci.*, **59**, 1913 (1996).
7. F.S. Bates, R.E. Cohen, and A.S. Argon, *Macromolecules*, **16**, 1108 (1983).
8. R. Greco, M.F. Astarita, L. Dong, and A. Sorrentino, *Adv. Polym. Tech.*, **13**, 259 (1994).
9. Z. Horak, J. Kolarik, M. Sipek, V. Hynek, and F. Vecerka, *J. Appl. Polym. Sci.*, **69**, 2615 (1998).
10. M. Fujiyama, *J. Appl. Polym. Sci.*, **63**, 1015 (1997).
11. H.I. Halimatudahliana and M. Nasir, *Polym. Testing*, **21**, 263 (2002).
12. S.-G. Lee, J.H. Lee, K.-Y. Choi, and J.M. Rhee, *Polym. Bull.*, **40**, 756 (1998).
13. M. Mucha, *Coll. Polym. Sci.*, **264**, 859 (1986).
14. R. Greco, H.B. Hopfenberg, E. Martuscelli, G. Ragosta, and G. Demma, *Polym. Eng. Sci.*, **18**, 654 (1978).
15. T.J. Nosker, D.R. Morrow, R.W. Renfree, K. VanNess, and J.J. Donaghy, *Nature*, **350**, 563 (1991).
16. M. Reading, *Trends Polym. Sci.*, **1**, 248 (1993).
17. G.M. Jordhamo, J.A. Mason, and L.H. Sperling, *Polym. Eng. Sci.*, **26**, 517 (1986).
18. P. Potschke and D.R. Paul, *J. Macromol. Sci. Part C - Polym. Rev.*, **C43**, 87 (2003).
19. O.O. Santana and A.J. Muller, *Polym. Bull.*, **32**, 471 (1994).
20. R.A. Morales, M.L. Arnal, and A.J. Muller, *Polym. Bull.*, **35**, 379 (1995).
21. E. Donth, *The Glass Transition: Relaxation Dynamics in Liquids and Disordered Materials*, Springer Verlag, New York (2001).
22. S. Matsuoka, *Relaxation Phenomena in Polymers*, Hanser, New York, (1992).
23. K. Ilsaka and K. Shibayama, *J. Appl. Polym. Sci.*, **22**, 3135 (1978).
24. Q. Yuan, W. Jiang, L. An, and R.K.Y. Li, *Polym. Adv. Tech.*, **15**, (2004).
25. L. Huang, Q. Yuan, W. Jiang, L. An, S. Jiang, and R.K.Y. Li, *J. Appl. Polym. Sci.*, **94**, 1885 (2004).
26. B. Ash, R.W. Siegel, and L.S. Schadler, *J. Polym. Sci.: Part B: Polym. Phys.*, **42**, 4371 (2004).
27. R. Gachter and H. Muller, *Plastics Additives Handbook*, Hanser Publishers, New York (1990).